T8:

Maser Astrometry *Chair: Huib Jan van Langevelde*

https://doi.org/10.1017/S1743921312007314 Published online by Cambridge University Press

Cosmic Masers - from OH to H_0
Proceedings IAU Symposium No. 287, 2012
R.S. Booth, E.M.L. Humphreys & W.H.T. Vlemmings, eds.

doi:10.1017/S1743921312007314

Maser Astrometry: from Galactic Structure to Local Group Cosmology

Mark J. Reid

Harvard-Smithsonian Center for Astrophysics, 60 Garden Street, Cambridge, MA 02138, USA
email: reid@cfa.harvard.edu

Abstract. This review summarizes current advances in astrometry of masers as they pertain to large-scale Galactic structure and dynamics and Local Group cosmology. Parallaxes and proper motions have now been measured for more than 60 massive star forming regions using the Japanese VERA array, the EVN and the VLBA. These results provide "gold standard" distances and 3-dimensional velocities for sources across the Milky Way, revealing its spiral structure. Modeling these data tightly constrains the fundamental parameters of the Milky Way: R_0 and Θ_0 . Proper motions of Local Group galaxies have been measured, improving our understanding of the history and fate of the Group.

Keywords. astrometry, masers, stars: formation, Galaxy: fundamental parameters, Galaxy: structure, Galaxy: kinematics and dynamics, galaxies: kinematics and dynamics, Local Group

1. Introduction

Figure 1 displays an image of NGC 1232, a galaxy classified SAB(rs)c that might resemble the Milky Way. It displays a multi-armed spiral with regular and bifurcated arms and a central bar, which may be weaker than in the Milky Way. Using NGC 1232 as a model for Milky Way, the Sun would be about two-thirds of the way from the nucleus to the edge of the stellar disk. The Hipparcos satellite measured $\sim 10^5$ stellar parallax with ≈ 1 mas accuracy and mapped the Solar Neighborhood. However, the Solar Neighborhood would cover an area not much larger than one of the H II regions that dot its spiral arms. Far better astrometric accuracy is needed to map the Milky Way.

The GAIA mission, scheduled for launch in 2013, hopes to achieve parallaxes to $\sim 10^9$ stars with accuracies of ≈ 20 μas. With this accuracy, one can measure a distance of 5 kpc with 10% uncertainty and begin to map large portions of the Milky Way. However, GAIA observes at optical wavelengths and will be limited to a small number of lines of sight in the Galactic plane owing to dust extinction. In order to map the spiral structure of the Milky Way, one needs observations at longer wavelengths. Very Long Baseline Interferometry (VLBI) at cm-wavelengths can accomplish this.

At cm-wavelengths dust in the Milky Way is transparent. VLBI parallax accuracy routinely is ~ 20 μas, and some measurements have achieved accuracies of 5 μas! Thus, one can measure distances to compact radio sources throughout the Galactic plane. Astronomical H_2O and CH_3OH masers are good astrometric targets and are found in regions of massive star formation. Such star forming regions are home to OB-type stars that ionize their placental material, and it is these H II regions that best define spiral structure in other galaxies. Thus, parallaxes of masers are an excellent method to map spiral structure in the Milky Way.

Figure 1. NGC 1232: a Milky Way look-alike?

2. VLBI Parallax Accuracy

While a thorough discussion of sources of error in phase-referenced VLBI astrometry is beyond the scope of this review, one can gain an appreciation of what is involved with $\sim \mu$as astrometry from a few key points. For a more thorough discussion see, eg, Honma, Tamura & Reid (2008) or Reid *et al.* (2009a).

The fringe spacing of a two-element interferometer is given by $\theta_f \approx \lambda/B$, where λ is the observing wavelength and B is the baseline length. For $B = 8000$ km and $\lambda = 1$ cm, $\theta_f = 250$ μas. The centroid position of a point-source imaged with a multi-baseline array with a FWHM beam size of $\approx \theta_f$ can be measured with a precision of $\approx 0.5\theta_f/\mathrm{SNR}$, where SNR is the peak signal-to-noise ratio in the image. Thus, even for modest SNR values of ~ 10, one can obtain a centroid positional precision of ~ 10 μas.

However, in most cases, systematic sources of error dominate and one's precision is far better than one's true accuracy. For observations at short cm-wavelengths, where *un-modeled* ionospheric delays are smaller than tropospheric delays, one can often achieve residual zenith path delay errors of ~ 1 cm. These un-modeled path delays are usually associated with large-scale irregularities in water vapor that change by ~ 0.5 cm per hour in a quasi-random-walk fashion. This level of zenith path delay noise can be achieved with regular measurement (via "geodetic blocks" or GPS data) and correction of the interferometer data. At a "typical" source zenith angle of 30°, this corresponds to ~ 2 cm of total path delay error. For an observing wavelength of 1 cm, this causes a $\sim 2\lambda$ shift in the optical path between antenna pairs, which can lead to a systematic shift of two fringes or about ~ 500 μas in the absolute position of a target. But, following a suggestion originally attributed to Galileo for parallax measurement, by measuring a *relative* position between a target and calibrator nearby in angle on the sky, this systematic position uncertainty can be largely canceled. For a typical target-calibrator separation of 1° (ie, 0.02 radians), one can achieve $\sim 500 \times 0.02 \sim 10$ μas accuracy.

3. Some Individual Parallax Results

One of the first high-accuracy parallax results was for W3OH. This source had a long-standing distance discrepancy: an optical photometric distance (assuming an association with O-type stars separated by $\sim 1°$ on the sky) gave 2.2 kpc, while a kinematic distance gave 4.3 kpc. Xu *et al.* (2006) observed 12 GHz (Class II) CH_3OH masers with the

https://doi.org/10.1017/S1743921312007314 Published online by Cambridge University Press

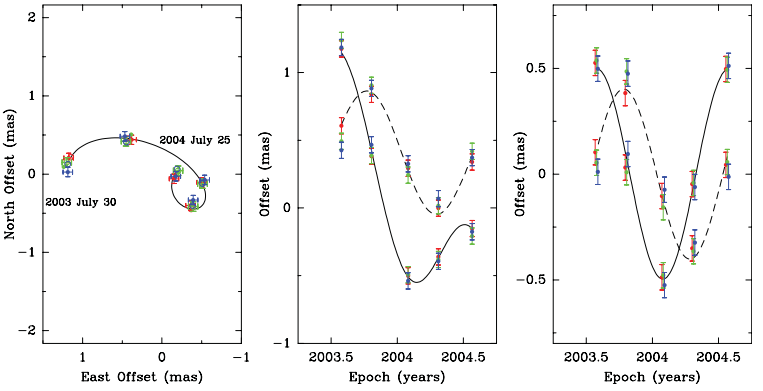

Figure 2. Parallax data for 12 GHz CH_3OH masers in W3OH from Xu *et al.* (2006). Left panel: positions on the sky of 1 maser spot measured relative to 3 background sources. Middle panel: eastward (solid line) and northward (dashed line) offsets versus time. Right panel: same as middle panel, but with proper motion removed, showing only the parallax signature.

Very Long Baseline Array (VLBA) and obtained a parallax of 0.512 ± 0.010 mas (see Figure 2). This corresponds to a distance of 1.96 kpc and indicates the photometric distance was accurate to about $\pm 10\%$. The measured proper motion indicates a peculiar (non-circular) velocity of 22 km s^{-1} largely toward the Sun, explaining the anomalous kinematic distance.

Honma *et al.* (2007) using the Japanese VERA array measured the first parallax for a distant, outer Galaxy source, S269 (see Figure 3). Their results confirmed the flatness of earlier rotation curve data well beyond the Solar Circle and, therefore, the need for substantial dark matter in the halo of the Milky Way. It is important to note that previous results, mostly using H I data were based on less reliable kinematic distances and only 1-dimension (radial) of velocity information. The VERA result was the first time that full 3-dimensional location and velocity information had been obtained for a distant outer Galaxy source.

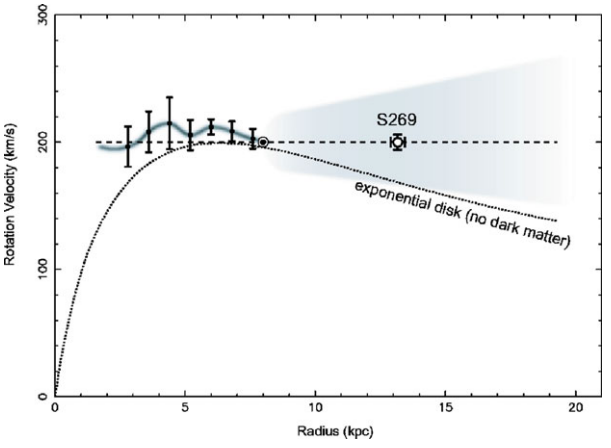

Figure 3. Galactic rotation curve including the VERA S 269 parallax and proper motion, indicating the need, from 3-dimensional data, for dark matter to sustain the rotation speed in the outer galaxy.

The 3-dimensional structure of the Cygnus-X region has been explored with European VLBI Network (EVN) observations by Rygl *et al.* (2011), who measured parallaxes for

https://doi.org/10.1017/S1743921312007314 Published online by Cambridge University Press

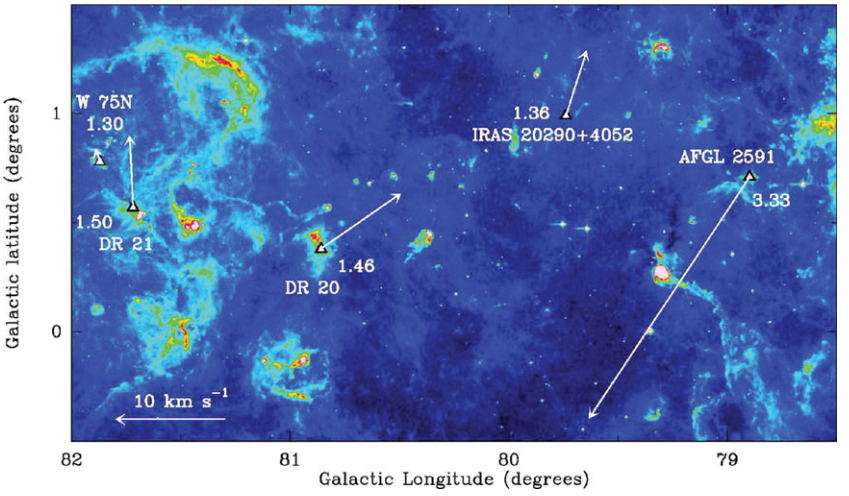

Figure 4. The Cygnus-X region from Rygl *et al.* (2011). Four sources are at a distance of ≈ 1.4 kpc; however AFGL 2591 is at 3.3 kpc and not associated with the "Cygnus-X" complex.

five massive star forming regions (see Figure 4). Four of these (W 75N, DR 20, DR 21 & IRAS 20290 + 4052) are consistent with being at a distance of 1.40 ± 0.08 kpc and are clearly associated with the same giant molecular cloud. However, one source, AFGL 2591, was found to be at a significantly greater distance (3.33 ± 0.11 kpc) and is not associated with the others. Thus, the Cygnus-X complex is not a single physical association. Toward this region one is looking down the Local Arm where multiple star forming regions are projected together.

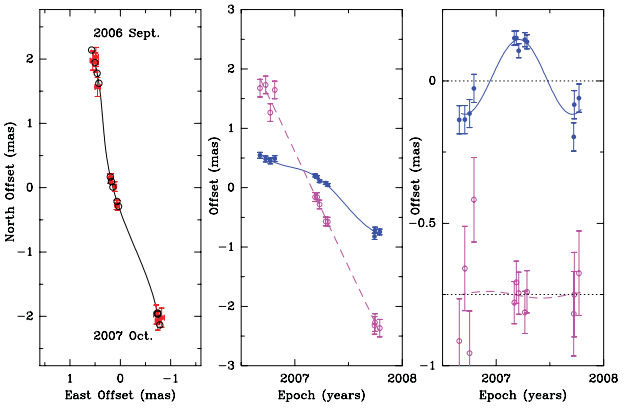

Figure 5. Parallax to the Galactic center source Sgr B2 from Reid *et al.* (2009c), yielding $R_0 = 7.9 \pm 0.8$ kpc. See Fig. 2 for a description of the plot.

Sgr B2 is located in the Galactic center region and is one of the most massive star forming regions in the Milky Way. Reid *et al.* (2009c) observed the H_2O masers in Sgr B2N and Sgr B2M and find a parallax of 0.129 ± 0.012 mas (see Figure 3), corresponding to a distance of 7.8 ± 0.8 kpc. While the line-of-sight distance from the Galactic Center (and its supermassive black hole Sgr A*) is unknown, Sgr B2 is probably ≈ 0.1 kpc nearer than Sgr A*. Evidence for this comes from i) Sgr B2's small projected distance of ≈ 90 pc from Sgr A* and ii) its 3-dimensional velocity (from the measured proper motion) which suggests a line-of-sight offset of 130 ± 60 pc (assuming a low eccentricity Galactic orbit)

https://doi.org/10.1017/S1743921312007314 Published online by Cambridge University Press

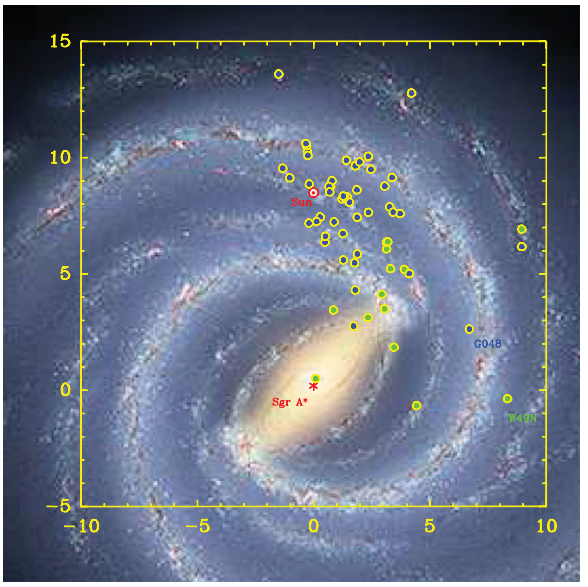

Figure 6. Locations of massive star forming regions with maser parallaxes measured by VERA, the EVN, and the VLBA overlaid on a schematic image of the Milky Way's spiral structure by R. Hurt. Blue circles are used when distance uncertainty is < 0.5 kpc, and green circles are used if the uncertainty is larger (typically three times the size of the circles). The spiral arm pitch angle plot (Fig. 7) suggests that G048 is associated with the Perseus arm and W49N with the Outer arm; hence the schematic image underlying the plot needs adjusting.

toward the Sun. Correcting for this small 0.1 kpc offset from the Galactic center gives a direct measurement of $R_0 = 7.9 \pm 0.8$ kpc. On going observations should yield a more accurate result.

4. Spiral Structure

Figure 6 shows the locations of 62 sources with parallaxes measured by VERA, the EVN, or the VLBA, overlaid on an artist's conception of the spiral structure of the Milky Way. Five sources (including W49; see the discussion of spiral pitch angles for justification for the arm assignment) now trace the Outer arm. Eleven sources (including G048) outline the Perseus arm, which is the arm nearest the Sun outside the solar circle. Moving inward, the Sun is embedded in the Local (or Orion) "spur." Inside the solar circle the definition of arms is less clear, especially as the sources approach the end of the bar near (3,3) kpc.

The Milky Way spiral arms might be approximated by a log-periodic function,

$$\log_{10}(R/R_{ref}) = -(\beta - \beta_{ref}) \ \tan\psi,$$

where R and β are the Galactocentric radius and azimuth and the subscript "ref" indicates reference values (eg, for the start of the arm). Such a spiral would map to a straight line on a plot of $\log_{10}(R/R_{ref})$ versus β, with slope given by $-\tan\psi$. The spiral pitch angle ψ controls how tightly wound is the spiral; values close to 16° (or 8°) would have arms wrap once (or twice) around the Galaxy before reaching the end of the stellar disk.

Figure 7 displays such a pitch-angle plot for sources with uncertainties in $\log_{10}(R/\mathrm{kpc}) < 0.1$ and uncertainties in $\beta < 10°$. Reid *et al.* (2009b), based on 5 sources in the Perseus arm, found $\beta \approx 16°$. Using this pitch angle (ie, holding the slopes constant)

https://doi.org/10.1017/S1743921312007314 Published online by Cambridge University Press

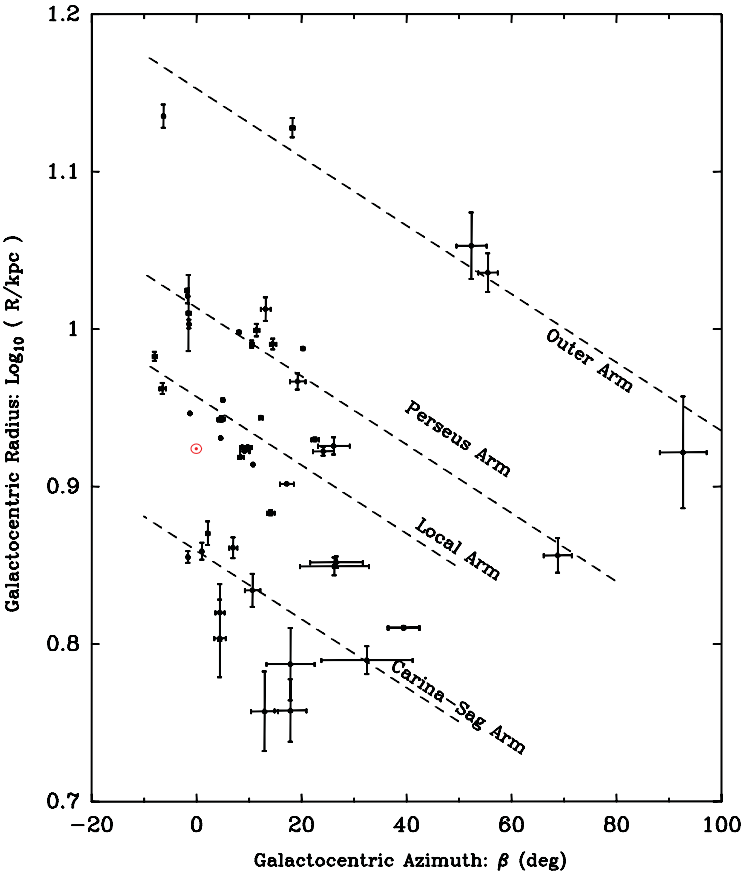

Figure 7. Spiral pitch angle plot. Plotted is the $\log_{10}$ of Galactocentric radius vs. Galactocentric azimuth; on such a plot, log-periodic spirals map to straight lines. The slope of the lines was fixed for a pitch angle of 16° from an analysis of 5 sources in the Perseus arm by Reid *et al.* (2009b); only a vertical offset was adjusted to better fit the data.

and adjusting only the vertical offsets for the lines in Figure 7, one can fit the data for the Outer, Perseus and Local arms reasonably well. (Interior to the Local arm, more data will be needed.) This leads to several interesting conclusions. Firstly, W49 at $(93°, 0.92)$ belongs to the Outer arm and G048 at $(69°, 0.86)$ belongs to the Perseus arm. Thus, the artistic conception of the Milky Way in Figure 6 needs to be adjusted. Secondly, the Local "spur" has a similar pitch angle as other arms, suggesting it is not a spur, which generally protrudes perpendicularly from an arm, and instead is a arm-segment. Thirdly, a globally averaged pitch angle value near 16° is generally characteristic of galaxies of Hubble type Sbc to Sc (Kennicutt (1981)).

5. Galactic Dynamics

With 3-dimensional position and velocity vectors for each source, one can construct an azimuthally averaged rotation curve for the Milky Way. For each source one must convert from the Heliocentric frame, in which the measurements are made, to a Galactocentric frame. This involves adding the full vector motion of the Sun in its Galactic orbit to each measured source vector and then calculating the projection of that vector in the direction of Galactic rotation. Figure 8 shows rotation curves generated for two values of Θ_0 (220

https://doi.org/10.1017/S1743921312007314 Published online by Cambridge University Press

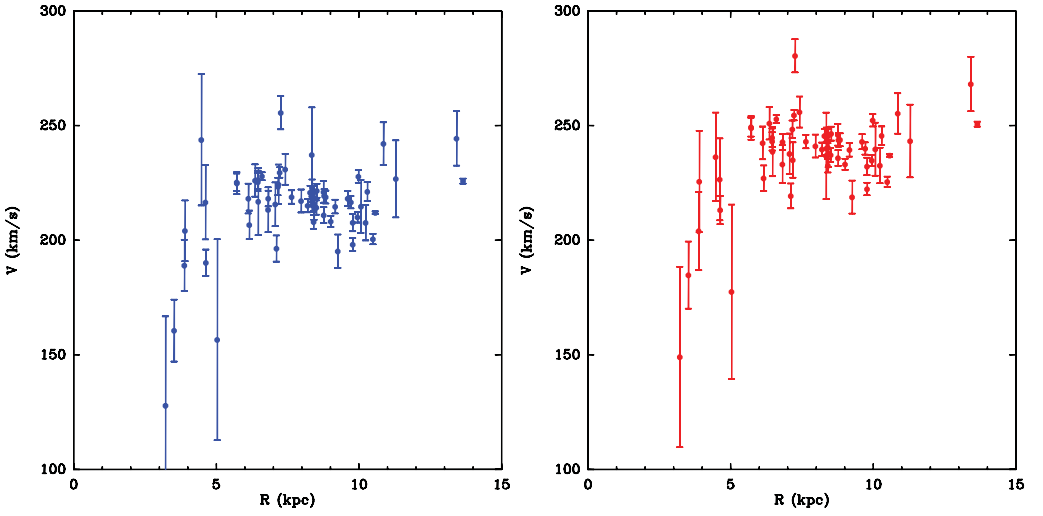

Figure 8. Azimuthally averaged rotation curves from the 3-dimensional data afforded by parallax and proper motion measurements. Left panel: used $\Theta_0 = 220$ km s^{-1} when converting from Heliocentric to Galactocentric (R,V) coordinates. Right panel: same as middle panel except $\Theta_0 = 245$ km s^{-1} was used.

and 245 km s^{-1}). Note the two curves resemble each other except for an offset of 25 km s^{-1}, corresponding to the difference in the two values of Θ_0. Thus, the average rotation speed seen in a rotation curve is essentially determined by the value of Θ_0 assumed when converting frames. Also, it is worth pointing out that all previous rotation curves were based on less reliable distances and only the radial component of the velocity vectors. Inferring Θ_0 from parallax and proper motions must come from modeling the entire data set, and not from the construction of an azimuthally averaged rotation curve.

Reid *et al.* (2009b) modeled the Milky Way using 18 maser parallax/proper motions and concluded that $R_0 = 8.4 \pm 0.6$ kpc and $\Theta_0 = 254 \pm 16$ km s^{-1} (adopting $V_\odot = 5$ km s^{-1} from Dehnen & Binney (1998)). A similar modeling of the 62 measurements can now be done. Using a "conservative formulation" of a Bayesian analysis described in section 8.3.1 of Sivia & Skilling (2006) that allows for outlying data, we find $R_0 = 8.5 \pm 0.3$ kpc and $\Theta_0 = 246 \pm 9$ km s^{-1}(adopting a new $V_\odot = 12$ km s^{-1} from Schoenrich, Binney & Dehnen (2010); using the older $V_\odot = 5$ km s^{-1} from Dehnen & Binney (1998) would give $\Theta_0 = 253 \pm 9$ km s^{-1}). Note that one expects the motions of some star forming regions to deviate from a simple model of Galactic rotation. The Galactic bar is known to cause large non-circular motions; also some sources may be affected by super bubbles from multiple supernovae and have sizeable peculiar velocities.

In addition, the new modeling confirms the conclusion of Reid *et al.* (2009b) that high-mass star forming regions lag circular orbits in the Galaxy, but by a smaller value of 6 ± 2 km s^{-1} if one adopts the updated solar motion.

6. Local Group Dynamics

In the 1920's, Adrian van Maanen reported measurement of proper motions of stars in the galaxy M 33. His motions were ~ 10 mas yr^{-1}, requiring that the "spiral nebula" M 33 was a Galactic object (to avoid $V > c$). van Maanen's motions were nearly a factor of 1000 too large and to this day the reason for the error lacks a clear explanation. A decade ago, Brunthaler (2004) for his Ph.D. thesis attempted to repeat the "van Maanen"

https://doi.org/10.1017/S1743921312007314 Published online by Cambridge University Press

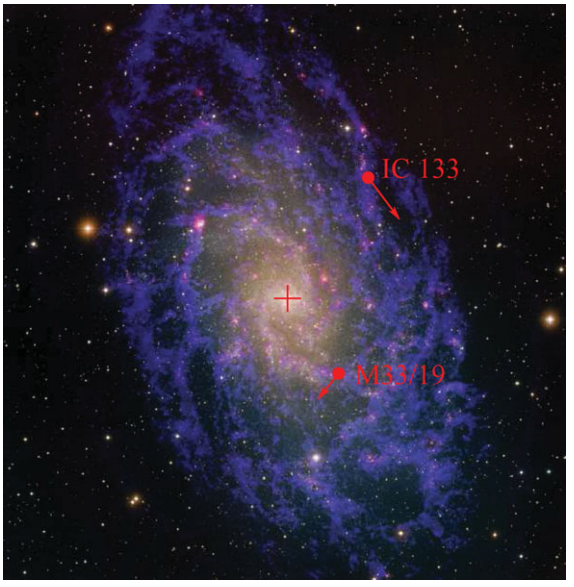

Figure 9. Image of M 33 with the locations and expected orbital motions of two H_2O masers. Credit: A. Brunthaler.

observations, using H_2O masers as astrometric targets. He succeeded both in measuring the internal rotation of M33 and its absolute motion across the sky relative to background quasars.

Brunthaler *et al.* (2005) compared the angular rotation of the H_2O masers with that predicted by the rotation speed and inclination of M 33 (determined from H I maps) and estimated the distance to the galaxy to be 730 ± 168 kpc. This was the first successful extragalactic "rotational parallax." With improvements in the observations (which are on-going) and in the rotation curve measurements, this geometric distance estimate can improve to better than 10% accuracy.

The absolute motion of M 33, a satellite of the Andromeda galaxy, also provides valuable information about the dynamics of the Local Group of galaxies. The Local Group is anchored by the Andromeda and Milky Way galaxies. We now know the 3-dimensional velocity of M 33 (relative to the Milky Way) and the radial velocity of Andromeda. Were we to know Andromeda's proper motion, we could integrate backwards in time and determine the history of the dominant galaxies of the Local Group. Constraints on the proper motion of Andromeda can be obtained from the measured velocity vector of M 33 and the fact that it hasn't been tidally heated by close encounters with Andromeda in the past. Loeb *et al.* (2005) rule out a null proper motion for Andromeda and suggest that its motion is probably near 100 km s^{-1}.

In the near future it will be possible to measure Andromeda's proper motion directly, owing to two recent developments. Firstly, after decades of searches for H_2O masers in Andromeda by several teams, Darling (2011), using the Green Bank Telescope (GBT), recently discovered 5 sites of H_2O masers in spiral arms that ring the galaxy. This will allow proper motion measurements similar to those done for M33, yielding both a rotational parallax and measurement of Andromeda's proper motion. Interestingly, Darling has noted that the "ring" of masers will *appear* to grow measurably in diameter over a decade as Andromeda approaches the Milky Way! Secondly, the recording rate will soon be 2 Gb/s on the VLBA. This increased bandwidth, coupled with the additional

https://doi.org/10.1017/S1743921312007314 Published online by Cambridge University Press

collecting area of the High Sensitivity Array (which adds 100-m class telescopes like the GBT, Effelsberg, and the phased-EVLA to the VLBA), will make it possible to directly measure the proper motion of M31* (the AGN of Andromeda). Indeed, a demonstration detection has already been accomplished (Brunthaler, private communication).

References

Brunthaler, A. 2004, *Ph.D. Thesis, Univ. Bonn*
Brunthaler, A., Reid, M., Falcke, H., Greenhill, L. J., & Henkel, C. 2005, *Science*, 307, 5714
Darling, J. 2011, *ApJ*, 732, L2
Dehnen, W. & Binney, J. J. 1998, *MNRAS*, 298, 387
Honma, M. *et al.* 2007, *PASJ*, 59, 889
Honma, M., Tamura, Y., & Reid, M. J. 2008, *PASJ*, 60, 951
van Maanen, A. 1923, *ApJ*, 57, 264
Kennicutt, R. C. Jr. 1981, *AJ*, 86, 1847
Loeb, A., Reid, M. J., Brunthaler, A., & Falcke, H. 2005, *ApJ*, 633, 894
Reid, M. J., Menten, K. M., Brunthaler, A., Zheng, X. W., Moscadelli, L., & Xu, Y. 2009a, *ApJ*, 693, 397
Reid, M. J. *et al.* 2009b, *ApJ*, 700, 137
Reid, M. J., Menten, K. M., Zheng, X. W., Brunthaler, A., & Xu, Y. 2009c, *ApJ*, 705, 1548
Rygl, K. *et al.* 2011, arXiv:1111.7023
Schönrich, R., Binney, J., & Dehnen, W. 2010, *MNRAS*, 403, 1829
&Sivia, D. S. with Skilling, J. 2006, *Data Analysis: A Bayesian Tutorial, 2^{nd} edition*, (Oxford University Press, Oxford UK), p. 168
Xu, Y., Reid, M. J., Zheng, X. W., & Menten, K. M. 2006, *Science*, 311, 53

https://doi.org/10.1017/S1743921312007314 Published online by Cambridge University Press